A review of Higgs boson pair production

Maxime Gouzevitch, Alexandra Carvalho

Reviews in Physics 5 (2020) 100039

Contents lists available at ScienceDirect

Reviews in Physics

journal homepage: www.elsevier.com/locate/revip

A review of Higgs boson pair production

Maxime Gouzevitch[a], Alexandra Carvalho*[,b]

[a] CNRS-IN2P3, Institut de Physique des Deux Infinis de Lyon, Universite de Lyon, Universite Claude Bernard Lyon 1, 2 rue Enrico Fermi Villeurbanne 69622, France
[b] NICPB Akadeemia tee, Tallinn 12611, Estonia

ARTICLE INFO

Keywords:
Higgs boson
LHC
ILC
FCC
CLIC
CEPC
Higgs potential
EWSB

MSC:
41A05
41A10
65D05
65D17,

ABSTRACT

In 2012 the ATLAS and CMS collaborations discovered at the LHC the Higgs boson decaying to vector bosons. This discovery has provided a strong indication that the mechanism of Electroweak Symmetry Breaking (EWSB) is similar to the one predicted by Brout-Englert-Higgs (BEH) nearly 50 years before. Since then, one of the priorities of the LHC program, as well as of the majority of the future collider proposals, is to measure directly the parameters of the EWSB potential. The goal is to identify if it has indeed the straightforward quartic shape predicted by BEH or it is more complex, as the result of an unexplored physics nature. The answer to this major scientific question will have a considerable impact on our understanding of vacuum properties and the history of the universe through the EWSB during the Big Bang. The only direct way to probe these couplings is through the measure of the production of multiple Higgs bosons, two being the simplest case. In this paper, we present a comprehensive review of the current searches and the state of the art insights on the topic. In particular, we explain why this ambitious project is even more challenging than the discovery of the Higgs boson itself. Finally, we sketch the plans of the HEP community for how to access the parameters of the BEH mechanism. This review is adapted to a curious reader familiar with particle physics in general or a scientist who wants to have a landscape overview of the topic.

1. Introduction: the brief history of mass

One of the first attempts that we know of a fundamental theory, including the concept of mass, is attributed to ancient Greeks. In their four-elements theory, the massive elements were Earth and Water, while Air and Fire were massless. The modern science, born with Galileo Galilei and Isaac Newton, separated the inertial mass, connected with the amount of force one needs to apply to accelerate an object and the gravitational mass that connects each object, including celestial ones, to the universal attraction force (gravity). The puzzling coincidence of inertial and gravitational masses was defined as the *Equivalence principle*. It was experimentally verified with higher and higher precision starting from Simon Stevin in 1586 and ending with the French satellite "Microscope" that quoted their identity up to 13 significant digits [1]! The Equivalence principle was the major brick of Einstein's theory of general relativity, *GR*. Gravitation was then transmuted from a Newtonian force with a "massive charge" into a geometric property of space deformed by the presence of massive objects.

The GR provided a macroscopic model of interaction between the mass of the objects and the space-time. It shall be noted that GR does not explain the origin of mass. This question had to be addressed within another framework, microscopic this time, the quantum field theory (QFT) and particle physics. The understanding of the force that binds together the nucleus of atoms (quantum

* Corresponding author.
E-mail addresses: mgouzevi@ipnl.in2p3.fr (M. Gouzevitch), alexandra.oliveira@cern.ch (A. Carvalho).

https://doi.org/10.1016/j.revip.2020.100039
Received 29 July 2019; Received in revised form 13 January 2020; Accepted 20 January 2020
Available online 18 February 2020

chromodynamics, QCD [2]) provided a microscopic explanation of 99% of the visible mass, that is the potential energy of the interaction between quarks and gluons confined in protons and neutrons. The remaining fraction was assigned to the rest invariant mass of up and down quarks, and electrons. Since further attempts to split quarks and electrons have failed at our energy scales, they can be considered as elementary particles. Meanwhile, two other elementary generations of heavy quarks and leptons were discovered. The span between the lightest charged elementary particle mass (electron with a mass of 0.0005 GeV), and the heaviest one (top quark with a mass of 175 GeV) is nearly six orders of magnitude. The neutrino masses are many orders of magnitude smaller than the electron mass. The origin of the mass of elementary particles and their hierarchy had yet to be discovered.

The idea of the Brout–Englert–Higgs mechanism (BEH) [3,4] was born to explain the origin of masses of the elementary particles. It is also connected with the success of the theory unifying two of the four known forces that act upon matter – electromagnetism and the weak force behind the Fermi theory of β decay. In this model, a primary electroweak (EW) interaction is spontaneously broken by the interaction with a BEH potential into an electromagnetic and a weak interaction. Massless photons mediate the electromagnetic interaction from one hand, and massive W and Z bosons mediate the weak interaction from the other hand. At the same time, the so-called Yukawa interaction of this potential with elementary fermions provided them with mass. All this theory is based on the existence of a fifth force, the BEH interaction, carried out by a new boson, the Higgs boson. That boson was discovered at the LHC in 2012 [5,6] and rendered a Nobel prize to Peter Higgs and Francois Englert.

The review is organized as follows: we start by briefly introducing the Higgs mechanism and the properties of the BEH potential. We explain why the shape of this potential is so critical and why its understanding is the next frontier of fundamental physics. In a second step, we describe the experimental techniques used since 2012 to measure the parameters of the BEH potential and explain why it is so complicated. Finally, we sketch how the scientific community plans to reach the required level of precision with the next generation of high energy colliders.

2. A note on theoretical aspects

In science, major theories are usually the outcome of a series of experimentation, failures and small successes attempted over time by large scientific communities. The construction and validation of the EW theory, resulting in the BEH mechanism, required nearly a century and is precisely of this kind. The framework behind this evolution is called quantum field theory (QFT), and it was developed during the beginning of the last century. In this framework, particles of matter are modeled as fields that couple with each other. The mathematical representation of the fields and their couplings are given in a function called a Lagrangian. The particles have an elementary quantum property called spin, with the dimension of rotational momentum and expressed in units of the Planck's constant. Particles with fractional spin are called fermions and compose the matter we know (quarks and leptons), and particles with integer spin are called bosons and are identified as carriers of the fundamental forces (for example, the gluon is the carrier of QCD). See, for example, the first chapters of Ref. [7] for a longer, but still accessible, description of some of the QFT concepts.

The basic ingredients of the EW theory were the description of both electromagnetism and the β decay [8] in the QFT language (respectively known as quantum electrodynamics, QED [9], and Fermi theory of Weak interactions [10]). Both theories were connected to the electric charge, and in that sense, it was appealing to try to unify them by a common description.

The solution for the unification of the QED with EW interactions followed a well-tested recipe. The EW theory was born as a description of the QED and the weak interaction as a unique EW field [11]. A striking difference had to be embedded into the new theory, though: QED has a macroscopic range, while the weak interaction a microscopic one, limited to act within atomic distances. A possible way out of this paradox was to admit that the Weak force is mediated by bosons with a mass significantly larger than the proton mass (around 100 times the proton mass), while the massless photon mediates electromagnetism. The problem, though, was that the introduction of explicit mass terms in the Lagrangian is not a good practice in QFT.

It has been known since the XIXth century that symmetries are valuable guidance principles to construct the description of interactions of matter and forces. One of the most important symmetries to be considered in QFT, that driven the introduction of the BEH mechanism [12,13] in the EW interactions is the so-called *gauge symmetry* [14]. A Lagrangian (description of the interactions between the fields) is defined as gauge-invariant if phase transformations in elementary fields do not change the form of their interactions. Fields that are gauge invariant (*i.e.* all interactions of this field are left intact by phase transformation) are observed as massless particles; the introduction of an explicit mass term breaks the gauge symmetry.

Guided by this principle, the BEH mechanism postulates a field (the Higgs field) that couples with the EW field. At high energy scales (above the TeV) both fields are observed as massless. At lower energy scales, the Higgs field self-interaction induces a spontaneous electroweak symmetry breaking (EWSB) of the Lagrangian gauge invariance. In the low energy regime, the theory naturally contains one massless boson (the photon, carrier of electromagnetism) and two massive vector bosons, one neutral (the Z boson) and one charged (the W boson). The W and Z bosons are the carriers of the weak force, and their existence was directly verified by experiments almost 20 years after the construction of the EW theory [15,16]. One of the many triumphs of the BEH mechanism was to predict the relations between the masses of the W and Z bosons at very high precision. As a side bonus, the Higgs field has a gauge-invariant coupling to fermions and, through the same EWSB mechanism, the masses of the fermions are generated without any *ad-hoc* violation of the gauge symmetry in the original theory. This construction implies the existence of another massive scalar boson in the low energy regime, the Higgs boson.

The model described above is so successful in making valid predictions that it is now known as the Standard Model of elementary particles (SM). A bit more technical review of the evolution of the construction of the SM is found, for example, in Ref. [17]. For almost a century, all the predictions of the SM have been again and again confirmed with high precision. The last discovery was the existence of a Higgs boson with a mass around the W and Z masses (known as the Weak scale) and all its properties matching the SM

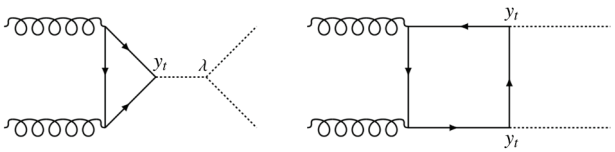

Fig. 1. The principal Feynman diagrams of the pair production of Higgs bosons via ggF. Left: Higgs self-coupling diagram. Right: top box diagram.

predictions. This observation is a solid hint toward the BEH nature of the EWSB. Still, the direct proof of the symmetry-breaking mechanism remains to be done.

2.1. The anatomy of double Higgs boson production

In the SM, the Higgs field potential is postulated to be a quartic potential (the lowest possible level for constructing a gauge-invariant Lagrangian). After EWSB, this results in a trilinear and a quadrilinear self-interaction to the Higgs boson in the low energy regime. The details of the EWSB mechanism and all the rich physics that is encoded in the Higgs field simple polynomial potential is very well described in Ref. [18]. For simplicity, we only describe the SM Lagrangian after the EWSB. In this case, the part of the SM Lagrangian that describes the Higgs boson interactions only reads:

$$L = \frac{1}{2}\partial_\mu \mathrm{H}\partial^\mu \mathrm{H} - V(\mathrm{H}) \tag{1}$$

where H represents the Higgs boson field, the first term is a derivative term that symbolizes the kinetic energy, the second is the term of the Higgs boson potential. After the EWSB the potential term can be written as:

$$V(H) = \frac{1}{2}\mathrm{m_H}^2\mathrm{H}^2 + \lambda\nu\mathrm{H}^3 + \lambda\mathrm{H}^4. \tag{2}$$

The second and third components of the potential represent the Higgs boson self-interactions, both are proportional to λ, the Higgs boson self-coupling constant. The ν in this term is a factor with the dimension of mass known as the Higgs field vacuum expectation value (vev). The first term in the equation above contains the mass of the Higgs boson itself, $\mathrm{m_H}$. In SM, there is a direct relation between the self-coupling constant, vev and the Higgs boson mass: $\mathrm{m_H} = \sqrt{2\lambda}\,v$. The Higgs boson mass ($\mathrm{m_H} \approx 125$ GeV) was measured with a sub-percent precision by the LHC, while the $\nu \approx 246$ GeV is constrained by the Electroweak precision tests of the Fermi theory with a precision of 7 digits [19]. Therefore if the Higgs boson potential that induces EWSB is exactly the one of the SM, we know that $\lambda \approx 0.13$ with a sub-percent precision. Any modification of the potential does modify this relation. The only way to answer the question of the exact structure of the BEH potential is to measure the Higgs boson self-coupling directly.

The lowest level Higgs boson self-interaction is the trilinear one (a coupling between three particles). The most promising and direct way to measure this coupling is through the detection of a pair of Higgs bosons in the final state. Unfortunately, the production rate of these events is about 1000 times smaller than that of the single Higgs boson, which makes its measurement at the LHC challenging. The description of this effort is the primary goal of this review. If we discover a self-interaction of the Higgs boson candidate different from the one predicted by the SM a major rethinking of the EWSB is required. This *ultimate* test of the SM predictions is at the center of the physics program of the LHC for next few years as well as of its subsequent project, the HL-LHC [20].

The LHC is a proton-proton collider, which smashes protons against each other at sufficiently high energy to induce interactions between elementary particles, allowing for the production of Higgs bosons. There are a few production modes for single and pair production of Higgs boson at the LHC: the leading one – gluon-gluon fusion (ggF), the associated production with vector bosons or top quarks, and the vector boson fusion (VBF). There is no direct coupling between Higgs bosons and gluons (those are massless), but gluons interact with quarks. Therefore, this process can only occur if mediated by a loop of quarks. The discovery of the Higgs boson was made in the ggF mode. Historically, this was the only particle to be discovered through a loop induced production mode.

All the fields in the SM, fermions or bosons, acquire their mass through their interaction with the Higgs bosons. The stronger the interaction is, the bigger the mass is. As the mass of the top quark is so big with respect to the other fermions (≈ 40 times more massive than the other heavier fermion, the bottom quark), it's coupling with the Higgs boson is the largest one, and we can assume that the particles in the loop are top quarks. The ggF production is therefore controlled by two parameters: the Higgs boson self-interaction (λ) and its coupling to top quarks (y_t).

In Fig. 1, we see a sketch of the principal Feynman diagrams[1] that contribute to gluon-gluon fusion production of Higgs boson pairs. On that figure, the curly lines represent gluons, dashed lines represent the Higgs bosons and the continuous lines the intermediary quarks. The Higgs self-coupling is pictured on the left. The dominant production mechanism on the right is mediated by a loop of top quarks (that looks like a *box*) and doesn't imply any Higgs self-coupling. The two kinds of processes in Fig. 1 interfere with each other to the point that deviations of either λ or on y_t result in sizable modifications of the predicted kinematic distributions [21].

If one stays with the SM parameters, the cross-section for the HH production and the kinematics of the Higgs bosons being produced is fully defined. The theory community provided us with high precision predictions of both, including significant QCD

[1] Richard Feynman introduced this schematic way of representing the interactions of the particles. The *x*-axis represents time, and the *y*-axis space. This diagram represents the sequence of connections and transformations between the particles over time.

corrections. This process was particularly challenging to calculate due to the presence of virtual corrections in a top quark box diagram [22]. The total uncertainty on the total cross-section, due to the missing orders in perturbative QCD, is estimated to be less than 10%. At the end of the game, the expected cross-section is too small to be measured with the LHC data collected between 2011 and 2018. That, however, does not discourage the deployment of the search with the intent of developing techniques to improve the sensitivity of the LHC to detect Higgs boson pairs.

2.2. And if SM is not all that is there

While any modification of the BEH potential with respect to the SM predictions is a clear indication that the SM is not a complete model, several beyond the SM (BSM) theories predict a modification of the BEH potential. Those can be observed as an anomaly in HH production. In some cases, the production rate can be enhanced by more than one order of magnitude, making the discovery (or the ruling out of the proposal) possible even today. There are two types of expected signatures in the HH final state that we briefly mention in the rest of this section. For a more detailed discussion see the Ref. [23].

The first type of anomalies is the easiest to detect, the production of a new massive particle that can decay to Higgs pairs, creating as its signature a distinguishable peak in the invariant mass of the Higgs boson pair. This process is called resonant production. Usually, those particles can also decay to vector bosons V or top quarks, also predicting resonant signatures in other detectable channels.

A particularly interesting class of theories that predicts resonant signatures in the Higgs boson pair production are the ones that postulate the existence of scalar singlets. Those scalar singlets can potentially mix with the Higgs boson and modify the BEH potential and the EWSB mechanism [24]. It is interesting to mention, however, its connection to cosmology. During the early times of the Big Bang, when our universe was significantly hotter than the TeV scale, there was no minimum in the BEH potential. The EW symmetry was preserved, and particles had no mass. When the universe cooled down, a non-trivial minimum appeared, and elementary particles acquired masses. The way that the universe passed between those states is called a phase transition. It may be soft, or second-order, like melting plastic, or violent, or first-order, like boiling water. In a first-order phase transition in some of the regions of the universe, particles have masses, while in some others they still do not. On the frontier of these domains, it is possible to generate a matter-antimatter asymmetry. Calculations show that with $m_H = 125$ GeV the SM predicts a second-order phase transition, but the modifications induced by a singlet can modify the phase transition properties. The best way to track this effect would be to look at the singlet coupling to HH. For more examples of models that predict resonant signatures, see, for example, the Ref. [25].

The second type of anomalies includes an extended Higgs sector. One of the most popular among them being the Minimal Supersymmetric Model (MSSM). In spite of having 'Minimal' in the name, that model predicts a rich Higgs sector, with two copies of the Higgs field as postulated in the SM. After EWSB the model contains seven Higgs bosons; some of those bosons are neutral and can mix with each other, generating both a modification of the self-coupling of the Higgs boson that was observed at the LHC (H) and the possibility of an extra Higgs boson (X) to decay into a pair of H bosons (see for example the Ref. [26]).

The second anomalous effect that could be discovered at the LHC sooner or later is the deviation of the Higgs boson couplings purely due to an extended symmetry of nature. In this case, the description of the low energy physics is done employing an effective model that is a reduction of a more fundamental one (known as an effective field theory, EFT). No resonance signature is predicted, the eventual additional particles that would participate in the model are too heavy to be directly observed in the energy regime that we can access experimentally[2].

For Higgs boson pair production, two relevant couplings are λ and y_t. Those are commonly parameterized by the factors $\kappa_\lambda \equiv \lambda_{BSM}/\lambda$ and $\kappa_t \equiv y_t^{BSM}/y_t$, where λ and y_t^{SM} are the values of those parameters as predicted by the SM (by construction, for the SM we have $\kappa_\lambda = \kappa_t = 1$). Furthermore, in EFT, new kinds of interaction can appear, for example, the contact interaction of one or two Higgs bosons with a pair of gluons and/or the contact interaction of two Higgs bosons to a pair of top quarks [28]. Any anomaly on the Higgs boson couplings and/or interactions causes modifications to the signature of the non-resonant production of Higgs boson pairs in the ATLAS and CMS detectors. An example of the phenomenology of such a case at the LHC can be found in Ref. [29].

3. Experimental results

The measurement of the production of pairs of Higgs bosons is a large scale scientific project that aims to extract a tiny signal from a large background. We can compare it to the well-known story of the search for the Higgs boson itself. At the time of the design of the LHC experiments ATLAS and CMS, the scientists were not aware of the Higgs boson mass and even of its existence. Precise EW fits based on the results from the previous generation of the experiments (LEP at CERN, Tevatron at Fermilab and SLC at SLAC) provided some hints that if the Higgs mechanism exists the Higgs boson mass shall be between 68 and 121 GeV at 68% CL [30][3]. In 2012 the ATLAS and CMS collaborations discovered the Higgs boson with a mass of 125 GeV, just at the edge of that window, corresponding to a 1 *sigma* deviation with respect to the EW fits.

There is a vast multiplicity of the possible production mechanisms at the LHC – ggF, VBF, associated production with a vector

[2] The EFT is a rather standard concept in physics [27]. The Fermi theory of the weak interactions is an EFT construction of the SM.

[3] The CL notation comes from Gaussian statistics. In a nutshell, the standard theory of measurements assumes the uncertainties to be Gaussian and defines Confidence Level (CL) intervals as regions where the truth shall be with a given probability. If we consider a Gaussian function of variance σ, the integrals between $-n\sigma$, $+n\sigma$ are called $n\sigma$ CL. For example $n = 1$ corresponds to 68% and $n = 2$ to 95%.

boson or a pair of b or top quarks — and decay channels of the Higgs boson – bosonic modes $H \to ZZ^*$, WW^*, $\gamma\gamma$ or fermionic modes $H \to b\bar{b}$, $\tau\tau$, $\mu\mu$ that could subsequently decay in a large number of final states. Many dozens of combinations of production mechanism times final state, each requiring a different analysis strategy, had to be considered at the same time by a large number of teams. The combination of all the obtained information subsequently lead to the discovery of this boson, the first characterization of its properties, and a firm indication that the BEH mechanism is responsible for EWSB. In summary, this project was an exceptional collective effort of many hundreds of scientists with a complex scientific and social structure.

The new quest for the BEH potential through the driving channel of double Higgs production has many similarities with the Higgs boson quest. The production mechanisms are similar, but the presence of two Higgses increases the number of relevant final states significantly. It also decreases by about 1000 times the cross-section, leaving rare production modes outside of the reach of the LHC program, unless interesting BSM effects enhance them significantly. Even the quest for the SM-like $gg \to HH$ production could appear at first glance desperate! It would have been indeed hopeless if we didn't know so much about the Higgs boson itself. Its mass, spin, parity, and main branchings provide a sturdy handle to tame down the backgrounds and combine different channels. The multi-particle final state of the HH decay provides a significant amount of information with complex correlations offering a perfect field for the usage of Machine Learning approaches (ML). To optimize the common tooling and theoretical interpretation the experimental and theoretical community self-organized into different structures[4] and counts in 2019 more than 200 working scientists.

3.1. The ATLAS and CMS experimental apparatus

In this review, we discuss the results from the proton-proton program of the LHC circular accelerator located at CERN near Geneva at the center-of-mass energy ($\sqrt{s}$) of 13 TeV. Two general-purpose detectors were built to collect the LHC collisions, ATLAS and CMS, with the Higgs boson discovery in mind. This is why the priority of their design was to provide an optimal measurement of photons, electrons and muons[5] with typical energies between 50-100 GeV produced by the decays of EW bosons, as well as the reconstruction of hadronic jets with an optimal ability to identify the ones that were initiated by b-quarks[6].

Both detectors look like giant barrels (ATLAS is 40 m in length and 22 m in diameter; CMS is 21 m in length and 15 m in diameter) closed by endcaps to cover nearly 4π in solid angle. Very schematically from the inside (closest to the interaction point) to the outside following a well known "onion-like" structure we find:

- A pixel detector able to identify the decay vertices of a B-meson efficiently and seed the charged particle tracks.
- A strip tracker detector that complements the pixel one but costs less and uses less energy to operate and produces fewer data.
- An electromagnetic calorimeter to measure and identify photons and electrons.
- A hadronic calorimeter to measure the energy of hadrons.
- A muon detection system.

Giant magnets provide a strong field ($\geq$ 2T) to bend the charged particles and to measure their momentum. The exact position and shape of the magnets differ for each experiment: in ATLAS, magnets have a weaker field, but particles follow a longer pathway, while CMS has a stronger magnet, but the detector itself is more compact.

The LHC machine provides over 40 million collisions per second, while the experiment's data acquisition system can afford to collect and write on tape only a few thousand events. Each event to be written consists of a list of outputs of hundreds of thousands of detector channels fired by the particles produced during the crossing of two bunches. The ATLAS and CMS collaborations have to face an outstanding challenge to skim out 99.99% of observed collisions and record only the tiny fraction of the most interesting events. The system designed to perform this task is called the trigger system. It is staged in two levels [31,32]. The first level trigger L1, composed of special hardware processors, relies on coarse information from the calorimeters and muon detectors to select the most interesting events in a time interval of few microseconds. It filters 100 kHz of events from the 40 MHz of collisions at the LHC. The high-level triggers (HLT) running on computer farms further decrease the event rate, from around 100 kHz to a few kHz, before data storage. The two-layer trigger system is efficient in selecting events with high energy flow, or those which contain photons or leptons from the EW probes.

Despite all technical differences, the final sensitivity of each detector for Higgs boson physics appears to be rather similar [5,6]. The detailed description of each detector can be found elsewhere [31,32].

3.2. Different final states relevant for HH search

In Fig. 2 we show different final states of the HH decay that could be observed during LHC collisions. Different probabilities are

[4] The CMS and ATLAS collaborations each created an HH dedicated forum, while the Higgs Cross Section Working Group, a CERN forum where theorists and experimentalists share ideas, have appointed a dedicated subgroup.

[5] In this section we denote both electron and positron (anti-electron) by the generic term 'electron' and muons and anti-muons by the generic term 'muon'.

[6] Of course the physics program of the general-purpose LHC detectors such as ATLAS and CMS wasn't limited by the 100 GeV scale physics of the EW bosons. Both detectors were also designed as wonderful TeV scale microscopes able to observe decay chains of heavy objects and perform high precision measurements.

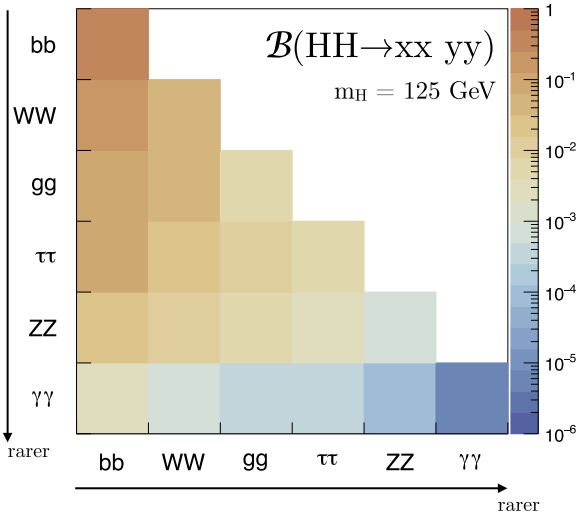

Fig. 2. Branching fraction of main HH decays assuming SM H boson.

provided assuming SM-like branching fractions. It was observed that four "golden" final states are much more sensitive than any others: HH→$\gamma\gamma b\bar{b}$, HH→$\tau\tau b\bar{b}$, HH→WW*$b\bar{b}$, and HH → $b\bar{b}b\bar{b}$. They are all localized in the first column of the plot and fulfill two optimal requirements for a successful search: one of the Higgses decays to a final state containing leptons or photons that are easy to trigger upon, to measure and hard to fake, while the other one decays to $b\bar{b}$ in order to maximize the total decay branching fraction[7].

There are standard steps common to all the HH searches that we describe below:

1. Identify and reconstruct all the particles produced by the HH decay under consideration.
2. Reconstruct when possible the invariant mass of each of the Higgs bosons.
3. Reconstruct and constrain the invariant mass of the two Higgs bosons, m_{HH}.
4. Reconstruct the angular distribution of the HH system: the production angle of HH, and decay angles of each Higgs boson.
5. Use the information obtained above to reject as much as possible the SM events that are not HH decays. The HH final state contains lots of information that usually allows filtering out most of the non-HH events, referred to as background.
6. Estimate the remaining background and look for the signal on top of it.

Below we describe in more detail the four golden final states and say a few words about the other ones (for a detailed discussion, see Ref. [23]). Each of the golden final states has its peculiarities, but one point in common, the H → $b\bar{b}$ leg. The model-dependent interpretation of the results is summarized in the Section 3.3.

3.2.1. HH → $\gamma\gamma b\bar{b}$

The HH → $\gamma\gamma b\bar{b}$ final state has the lowest branching fraction compared to the three other channels (only 0.26%), but the final state can be fully reconstructed and can be easily separated from other SM processes that play a role of background in this analysis.

The two isolated photons from the Higgs boson decays carry a typical transverse momentum of $m_H/2 \approx 60$ GeV. They are convenient to identify as two compact deposits in the EM calorimeter separated from other deposits by a region of minimal calorimetric activity. It is possible to build a trigger that collects nearly all events containing such pairs of photons within the acceptance of the detector.

In Fig. 3, we represent on the left the Feynman diagram for the HH → $\gamma\gamma b\bar{b}$ signal and on the right the main background. In this example, two b-quarks are produced by a QCD interaction between two protons followed by a subsequent QED radiation of two photons (referred to as QCD + QED background). We may observe that both final states are identical, and for this reason, the QCD + QED background is called "irreducible"[8]. The only way to separate such backgrounds relies on kinematical constraints.

The invariant mass of the two photons, $m_{\gamma\gamma}$, is a precisely measured quantity with a resolution of around 1-2%. The Higgs boson appears as a narrow peak on top of the QCD + QED background, which doesn't exhibit any peaking structure, as shown in Fig. 4 (left).

The invariant mass of the H → $b\bar{b}$ leg is another well-discriminating variable between the signal and the nonresonant background. The b-quarks hadronize into meta-stable B mesons and decay via EW interaction to lighter mesons and neutrinos. All the resulting flow of

[7] The HH → $b\bar{b}b\bar{b}$ does not fulfill this condition, but it has numerous compensating advantages that we discuss in a dedicated subsection.

[8] It is interesting to notice that a small irreducible background is the single Higgs production together with two b-quarks. We face here an analysis where Higgs boson production is a background and not a signal.

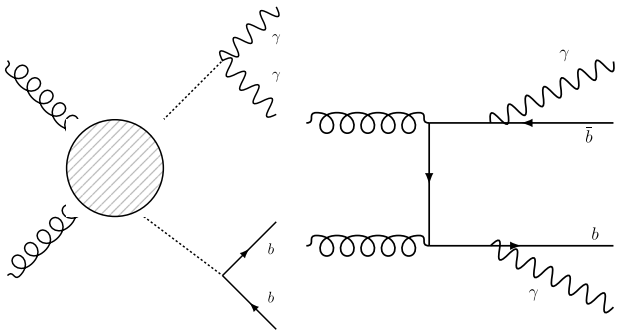

Fig. 3. The Feynman diagrams for the signal (left) and main QCD + QED background (right).

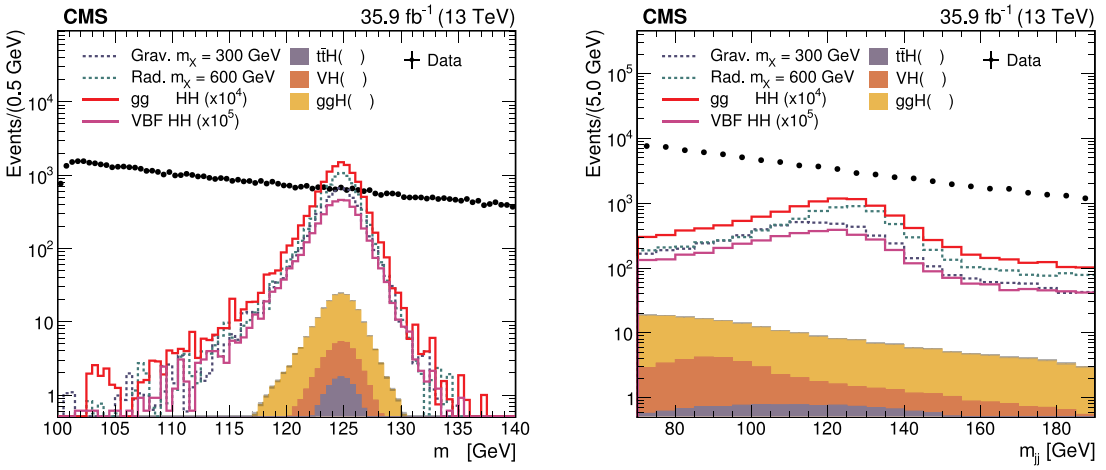

Fig. 4. The HH → γγbb̄ signal hypotheses scaled by factors indicated in parantheses (colored lines), CMS data dominated by the QCD + QED background (black points) and rare backgrounds (colored histograms). The $m_{\gamma\gamma}$ spectrum is shown on the left and m_{jj} on the right (see Ref. [33]).

particles is reconstructed as a hadronic jet in the detectors. Within this jet, the decay point of the B meson is usually displaced by a few mm in the transverse direction from the *pp* interaction point. The pixel detectors of the ATLAS and CMS collaborations are optimized to measure this displacement and identify rather rare b-quark generated jets from much more frequent jets produced by light quarks.

The invariant mass of the two jets, m_{jj}, is measured with a typical resolution of 10-20%, which is an order of magnitude worse than the diphoton one (see Fig. 4, right). In contrast to a photon, which is a point-like particle, a jet is a flow of different particles with a rather broad energy spectrum. Some of them might be soft and not well reconstructed by the detector. The B-meson decay products frequently contain neutrinos, which take away a significant fraction of the jet 4-momentum but escape the detector volume unseen. A dedicated jet energy calibration team is working to improve the understanding of the jet energy resolution continually and to improve it.

In practice the CMS collaboration looks at distributions of $m_{\gamma\gamma}$ and m_{jj} to identify the signal [33]. The ATLAS collaboration prefers to look on $m_{\gamma\gamma}$ and cut on m_{jj} [34]. The remaining kinematical variables, such as angles or particle momenta that allow separating the signal from SM background, are embedded into an ML or selection-based classifier. This classifier is subsequently used to identify regions in the kinematic phase space with maximal signal over background ratio.

3.2.2. HH → ττbb̄

This final state differs from the previous one by the presence of two τ leptons instead of two photons. It has a much more significant branching fraction (7.3%), but taus appear as more complicated objects to reconstruct and identify than photons.

The τ lepton (mass 1.8 GeV [35]) is the heaviest of all leptons. It can decay via the charged weak current to a ν_τ neutrino accompanied either by lighter leptons in ≈ 40% of cases (μ or e), or light hadrons (typically 1 to 3) in 60% of cases. Therefore a τ either appears as a lepton with missing momentum (so-called leptonic τ, denoted τ_l) or as a narrow jet (so-called hadronic τ, denoted τ_h[9]). A rather sophisticated ML algorithm is required to identify the τ_h and reject hadronic jets that look like taus.

[9] In fact experimentally τ_h are fascinating objects because they come from a color singlet lepton and are characterized by a tiny number of well-identified hadrons. In CMS, for example, their identification was one of the motivators to develop the Particle Flow algorithm combining all the information from all the detectors together [36].

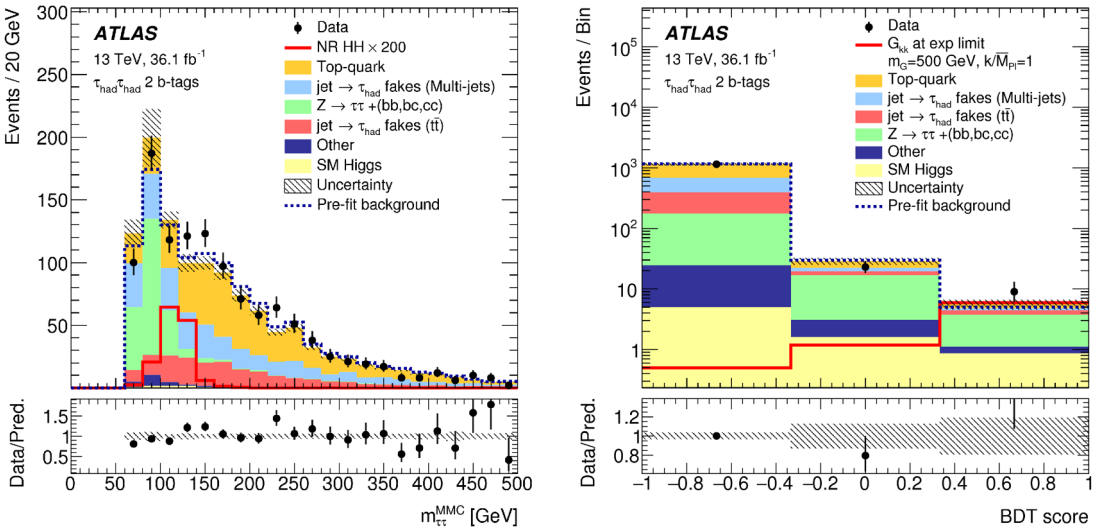

Fig. 5. The HH → ττbb̄ signal hypotheses (red line), ATLAS data (black points) and backgrounds (colored histograms). The $m_{\tau\tau}$ spectrum is shown on the left and the output of the BDT training on the right (see Ref. [37]).

There are six different combinations that one can observe in H → ττ decay: $\tau_h\tau_h$, eτ_h, $\mu\tau_h$, eμ, $\mu\mu$, and ee. The first one is privileged by decay branching fraction, the second and third are easier to trigger upon using the light leptons signature, the last ones suffer from a low branching fraction.

The presence of neutrinos, which cannot be detected, requires a mathematical procedure, called kinematic fit, to reconstruct H → ττ mass. One needs to combine the visible mass of a specific τ with an estimate of the momentum of the neutrino coming from the transverse momentum conservation laws. The τ leptons from Higgs boson decay are always produced with high momentum due to a vast difference in scale between Higgs energy and the τ mass. Consequently, we can assume that the neutrinos are collinear with the visible products of the τ decay. In the end, the fitted di-tau mass, $m_{\tau\tau}$, has a similar resolution to m_{jj}. It is shown in Fig. 5 (left) where one can observe that the broad $Z \to \tau\tau$ and H → ττ peaks overlap significantly.

The two main backgrounds for this final state are $Z \to \tau\tau$ production accompanied by two b-jets, and tt̄ production with subsequent decays to b quarks, leptons, and neutrinos[10]. Since the Higgs masses in the case of this analysis are not so discriminating, the CMS collaboration uses for the signal search variables related to the mass of the HH system built from two τ's and two b-jets [38]. The ATLAS collaboration uses directly the ML analysis output to discriminate signal from background [37]. An example of such an output is shown in Fig. 5 (right). It is defined in such a way that the signal is clustered around 1 and the background around -1.

3.2.3. HH → WW*bb̄

A W boson can decay or to a lepton and a neutrino either into two jets. The former is less frequent, but the overwhelming QCD dijet production challenges the latter. It had been observed that the final state with WW* → $ll\nu\nu$ (referred to as fully leptonic), where l is an electron or muon, has better sensitivity to SM-like production than the final state with hadronic decays (semi-leptonic or fully hadronic).

The fully-leptonic search has many similarities with the HH → ττbb̄ analysis. The unique relevant and irreducible background is the tt̄ production sketched in Fig. 6. The search for HH production in this channel becomes a high precision comparison of data vs. tt̄ production, which is rather well described by Monte Carlo (MC) predictions[11].

The H → WW* invariant mass cannot be reconstructed. The W mass (≈ 80 GeV) is close to the Higgs mass, and one of the W bosons (or both) is off-shell[12], and therefore we cannot use the same collinear approximation as for τ's. The analysis needs to rely more heavily on a multivariate discriminant. The latest LHC results regarding the fully-leptonic channel can be found in Refs. [39,40] and for the semi-leptonic in Refs. [41,42].

3.2.4. HH → bb̄bb̄

Similarly to HH→$\gamma\gamma$bb̄, this final state is fully reconstructible. On top of that, the branching fraction is as high as 33%. The

[10] The top quark is the heaviest known elementary particle. It decays through the weak interaction nearly exclusively to Wb [35], before any color confinement process could start.

[11] The MC simulation is a generic term to describe all the techniques that try to reproduce reality using a random generator, like in Monte Carlo casinos.

[12] In quantum mechanics, the mass of an unstable resonance is not well defined by the Heisenberg principle. There is a mass probability distribution with a width Γ, peaking at the so-called "pole mass". This pole mass is usually called "resonance mass". A resonance with a mass close to its pole mass is said to be "on-shell". If the mass is different from the pole mass by a few Γ the resonance is said to be "off-shell".

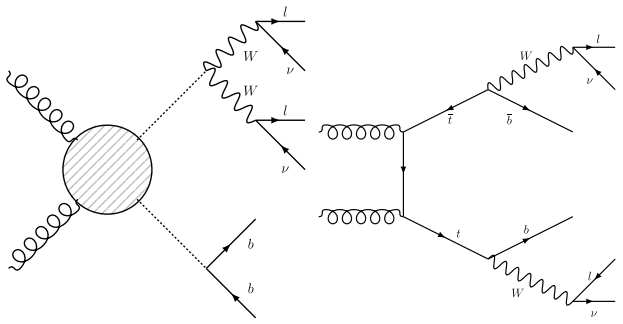

Fig. 6. The Feynman diagrams for the HH → WW*bb̄ signal (left) and the main tt̄ background (right).

drawback is the lack of objects that are convenient to trigger on, such as photons or leptons. Moreover, the multijet final states can be profusely produced by the QCD interaction without any EW contribution.

The choice of a good trigger is, therefore, critical to select signal events while keeping the data collection rate acceptable. The presence of four jets can be easily detected, but without a possible identification of their B-meson content since the actual trackers are too slow to participate in the L1 trigger. Jets with B-mesons can be identified in the HLT computing farm. There are two typical situations to consider. When the m_{HH} value we are interested in is typically below 500 GeV (low mass resonances or nonresonant search), the specific trigger for HH → bb̄bb̄ requires at the L1 trigger an optimal selection of the 4-jets with maximal p_T and some acceptance constraints. At the HLT ideally, two of the jets should be b-tagged. When $500 < m_{HH} < 900$ GeV, the trigger rates are lower and the online b-tagging constraints can be relaxed.

The signal extraction method is defined by our ability to estimate the substantial QCD background. This background is not well described by MC simulation due to significant higher-order corrections in perturbative QCD. Analyzers need to invent intricate data-based methods to estimate it. The method depends on how the trigger is constructed and in that sense, is very different in ATLAS and CMS [43,44]. The former relies on the m_{HH} distribution to separate data from MC, while the latter uses an ML output distribution for the same purpose.

3.2.5. Other processes

Many other channels were considered for this search: HH → ZZ*bb̄ → 4lbb̄, HH → 4τ, HH → 4W, HH → 4γ, HH → WW*γγ [45]. All those final states are very rich in leptons and photons and cannot be easily faked by SM processes. Also, the background is typically very low, giving essentially close-to-zero background searches. Unfortunately, they are severely penalized by their branching fractions (see Fig. 2) and at the end, appear to be less sensitive than the four golden channels. There is significant analysis work ongoing to see if some of them can still be improved or used for searches within the BSM Higgs models, where the Higgs branching fractions are different from the SM and more favorable for these final states.

3.3. Results

No HH signal has been observed in data as of this writing. We discuss different results of the LHC searches looking at the 95% confidence level (CL) exclusion limits assuming different BSM models predicting resonant and nonresonant anomalous HH production.

3.3.1. Resonant searches

The limits on the production of heavy resonances *X* with subsequent decay to HH are considered for generic models. They are defined in a way to bridge the interpretations in different BSM extensions of the SM. From the experimental point of view, a generic bosonic heavy resonance is defined by:

- Production mechanism: quark-quark fusion or Drell-Yann (DY), ggF, or VBF. In models where *X* decays a significant fraction of the time to Higgs bosons, the couplings to light quarks are suppressed. This fact disfavors the DY production mechanism and usually favors the ggF process.
- Mass: to produce two H bosons in the final state, one needs $m_X > 2m_H$.
- Width: if the natural width of a resonance is smaller than the experimental resolution, we can neglect it. This assumption is called the *narrow width approximation*. For $m_X < 1$ TeV the narrow width approximation holds for a large fraction of BSM models. In case it doesn't hold, we shall consider in the future limits for different width assumptions, intermediate and wide.
- Spin: scalar – spin-0, vector – spin-1 or tensor – spin-2. The decay of a spin-1 resonance to a pair of Higgs bosons is forbidden at tree level, and only spin-0 or spin-2 are considered.
- Parity: in our case, the system of two Higgs bosons has parity +1. Only an *X* with parity +1 can decay into HH – for example scalars can (spin-0, parity +1), while pseudo-scalars (spin-0, parity -1) cannot.

In Fig. 7, we show an example of the limits set for the resonant production of a heavy and narrow spin-0 resonance *X* with

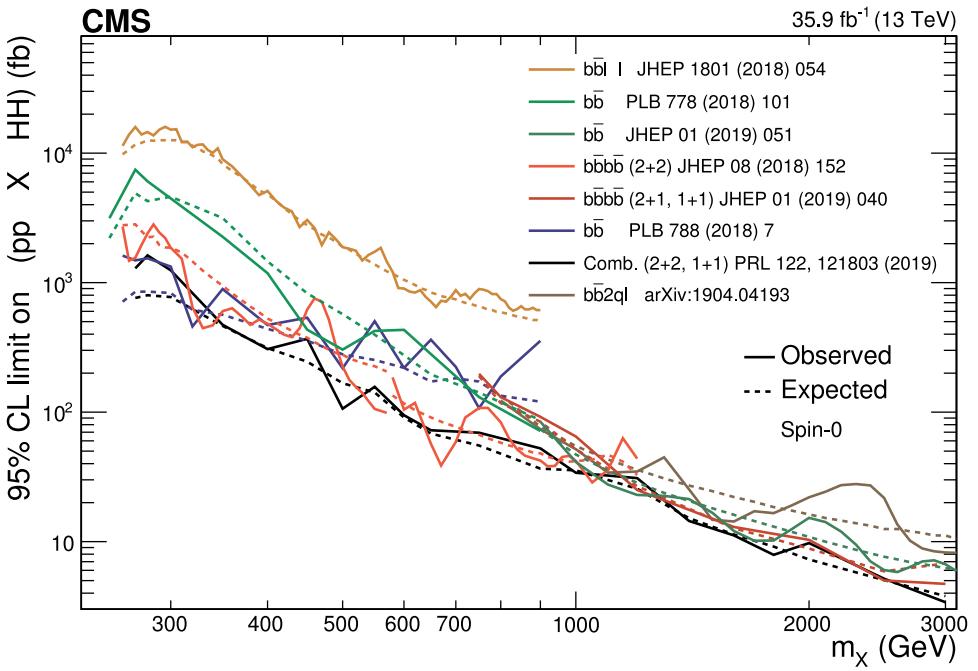

Fig. 7. Cross section values excluded at 95% confidence level by the CMS collaboration for a spin-0 resonance produced in a narrow width approximation (see Ref. [23]).

subsequent decay to HH split into different final states, taking the results of the CMS collaboration as an example. At low mass, $m_X < 400$ GeV, the particles from HH decay are relatively soft. The most sensitive channel is then HH → $\gamma\gamma b\bar{b}$ since photons are the easiest objects to trigger on and to reconstruct. In the high mass regime ($m_X > 700$ GeV), the objects to be measured have higher momenta and can be easily triggered upon. Therefore the channels with the best branching fractions, HH → $b\bar{b}b\bar{b}$ and HH → $\tau\tau b\bar{b}$ provide the most stringent limits. The HH → WW*$b\bar{b}$ remains for the moment the less sensitive among the four golden final states due to the overwhelming and irreducible $t\bar{t}$ background. The combination of all channels improves the individual limits significantly since at any value of m_X, except the region around $2m_H$, at least two channels significantly contribute to constraint the BSM production.

The excluded cross-section by itself doesn't tell much about the impact of HH searches on the BSM physics. We shall consider explicit models and see how much our results constraint their parameter space. For example, on the already mentioned MSSM, there is a small region between $2m_H \approx 250$ GeV and $2m_{top} \approx 350$ GeV where the lack of HH resonances in actual data excludes a significant region of the phase space of the model, as shown in Fig. 8 (left)[13]. It is interesting to notice that this region corresponds to the crossing of sensitivities of different HH channels (see Fig. 7), and the combinations of them help a lot to improve this constraint. The impact of the LHC results on the singlet model described in Section 2.2 is shown in Fig. 8 (right). The data are not yet able to exclude the cosmologically relevant parameters of the singlet models shown by the red dots, but the HL-LHC program may exclude or observe a large fraction of the parameter space.

3.3.2. Nonresonant searches

If the resonance *X* is too heavy (typically heavier than a few TeV), this resonance cannot be directly observed at the LHC[14]. The laws of quantum mechanics still allow observing the effects of such resonances through the modification of the HH cross-section or the deformation of the m_{HH} shape. For example, *X* can be produced off-shell with a mass lower than the pole mass, or contribute to loop-induced processes. Experimentally, events with different m_{HH} values would have a different efficiency due to trigger effects, events selections, and detector acceptance. Therefore nonresonant BSM effects cannot be explored in a model-independent way. One has to assume a particular m_{HH} spectrum to perform the search[15].

The simplest assumption consists of admitting that the m_{HH} spectrum is SM-like, but the total cross-section is unknown. This ggF

[13] The MSSM has many fundamental parameters, and an interpretation requires assumptions about the relations among them. The model proposed in Fig. 8 is called *hMSSM* since it assumes that the lightest neutral MSSM Higgs boson is the particle that was discovered by the LHC at the mass of 125 GeV [46].

[14] The probability of producing a resonance in *pp* collision rapidly decreases with m_X. This observation can be explained by the fact that the collisions do not occur between protons themselves but between their constituents quarks and gluons that carry a fraction of the proton's momenta. The probability of finding a constituent of the proton carrying a substantial fraction is prohibitively small. So even if it is possible to produce a resonance with m_X of few TeV in a collider with $\sqrt{s} = 14$ TeV, the probability of this phenomenon is negligible.

[15] A proposal on how to construct a more model-independent approach was made in [48].

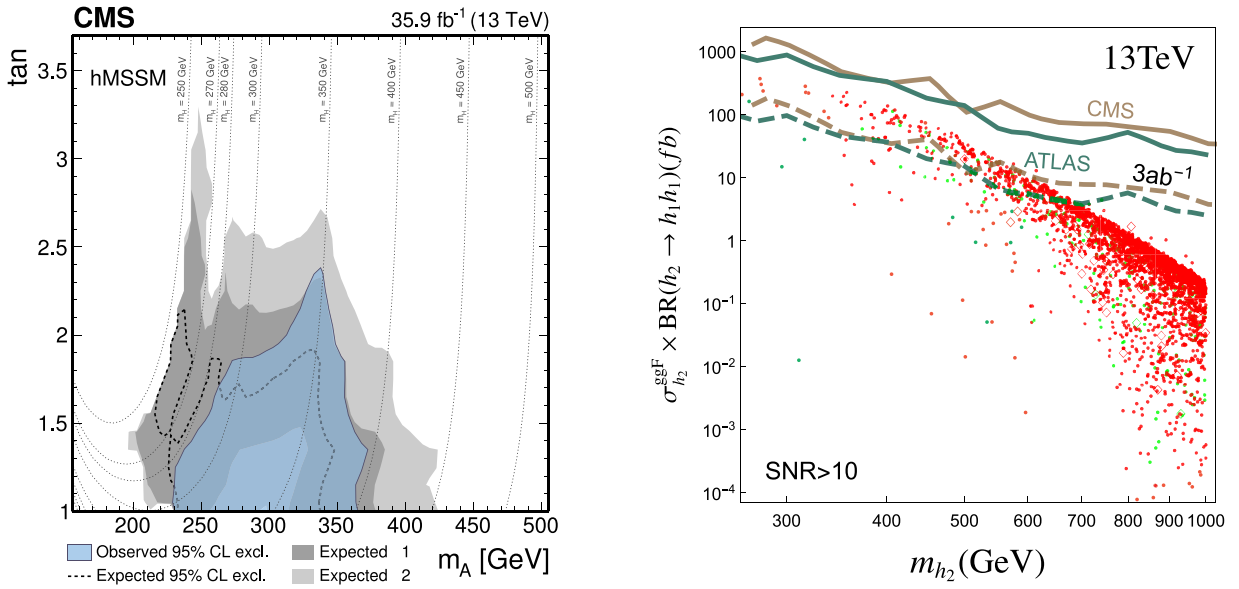

Fig. 8. Left: Excluded region of the hMSSM phase space obtained using the limits of the $X \rightarrow HH$ production for the parameter space constrained by the presence of a Higgs boson with a mass of 125 GeV (see Ref. [38]); Right: points of the model postulating the existence of an extra singlet that could generate gravitational waves observable by the future Laser Interferometer Space Antenna (LISA). The LHC limits are shown with full lines and the HL-LHC ones with dashed lines (see Ref. [47]).

spectrum, shown in Fig. 9 by the green dashed line, is peaking around $m_{HH} = 400$ GeV. A top quark box mediates one of the Feynman diagrams contributing to the ggF process (see Fig. 1) and when the m_{HH} mass exceeds the $2m_{top} \approx 350$ GeV threshold the production probability increases. It decreases eventually due to the decreasing probability of finding two gluons with high momentum inside the protons. These kinds of peaks that are not produced by an on-shell resonance but rather by a combination of phase-space factors are called *kinematic peaks*.

We have seen previously that three of the golden channels are nearly equally sensitive to a resonance produced with $m_X = 400$ GeV. We expect therefore a comparable sensitivity of those channels to SM-like production and a significant improvement from their combination. The results from the ATLAS and CMS collaborations are shown in Fig. 10. This kind of anomalous production is excluded with a cross-section larger than 7 times the SM one [49] by the ATLAS data. The CMS results are more permissive and allow cross-sections below 22 times the SM [50]. Both collaborations have a similar experimental reach, but in nearly all CMS channels, there is an upward fluctuation of data above the SM backgrounds and in the case of ATLAS analysis the opposite occurs. This situation is statistically possible and would certainly evolve when the 3 times larger data sample from Run II on the tape is analyzed.

To probe BSM physics in the nonresonant search the ATLAS and CMS collaborations use the EFT approach, which predicts an

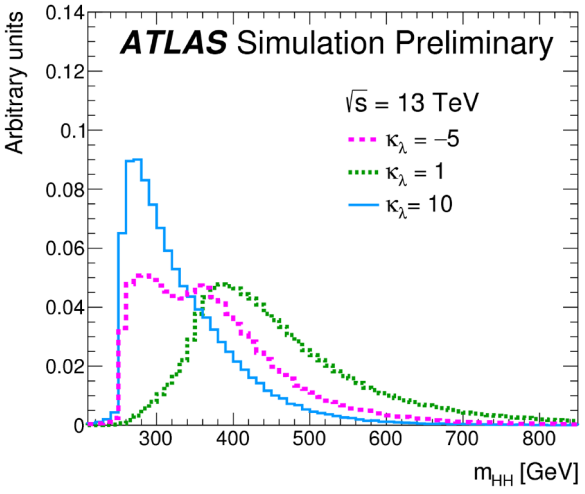

Fig. 9. The m_{HH} spectra for different assumptions on κ_λ (see Ref. [49]).

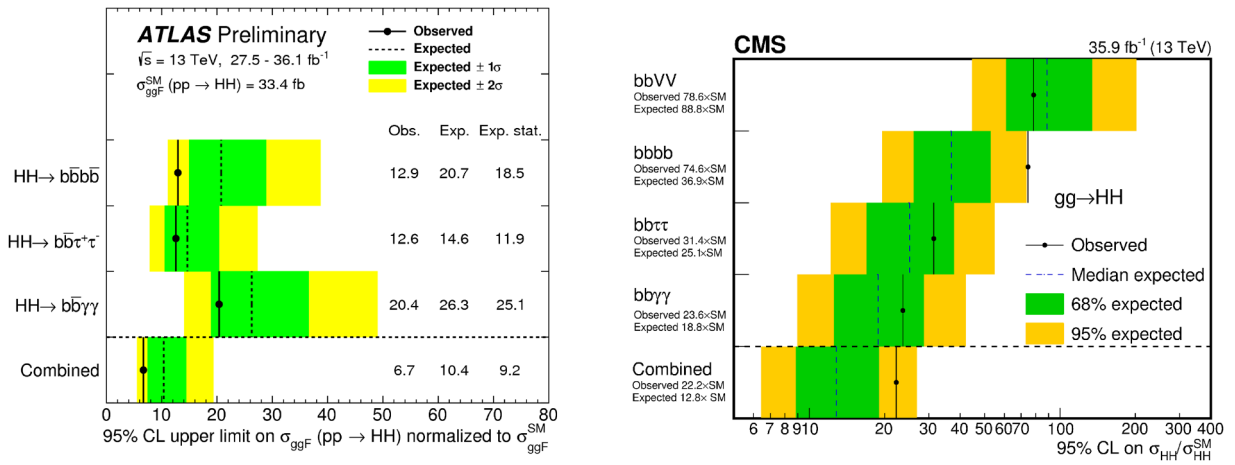

Fig. 10. Cross section values excluded at 95% confidence level in units of SM cross section by the ATLAS (left) and CMS collaborations (right). (see Refs. [49,50]).

independent modification of the Higgs couplings (see Sec. 2). As a first simplification, modifications of only the top Yukawa and Higgs self-couplings are considered. The top Yukawa coupling is directly constrained within 40% of the SM value by the tt̄H production rate recently discovered by LHC collaborations [51,52]. This constraint is direct and significantly better than what one can expect from the HH production. So in a further approximation, we can try to derive the constraints on the self-coupling parameter, κ_λ, assuming $\kappa_t = 1$.

Limits in κ_λ are shown in Fig. 11 for the ATLAS and CMS collaborations. To understand the features of the limits, we shall look again at the m_{HH} shapes for different κ_λ values shown in Fig. 9. We can see that for $|\kappa_\lambda| > > 1$ the kinematic peak shifts from 400 to 270 GeV. For these κ_λ values, the self-coupling diagram from Fig. 1 is dominating over the box diagram. The Higgs boson in the propagator of $gg \to H^* \to HH$ has to be significantly off-shell. The minimal possible mass of the propagator is just above $2m_H \approx 250$ GeV. From the resonant search, we have seen that the most sensitive channel in this region of m_{HH} is $HH \to \gamma\gamma b\bar{b}$. For these large κ_λ values, the m_{HH} shape (and the limit) is rather independent on κ_λ, while the cross-section evolves as κ_λ^2. Around $\kappa_\lambda \approx 1$, the kinematic peak is higher in energy and the sensitivity is larger, but, due to strong interference effects between the box and triangle diagrams, the cross-section is even smaller. Both experiments provide a rather loose constraint at κ_λ, and the best one is $[-5, 12]$, driven by the downward fluctuation in ATLAS data. Much more data from future collider programs would be needed to pin down κ_λ if its value is close to the one predicted by the SM.

4. Constraints on anomalous HH production from future colliders

The quest for the direct measurement of the parameters of the BEH is central for most of the future colliders. It is usually expressed as the possible constraints in κ_λ assuming all other EFT parameters to be at their SM value.

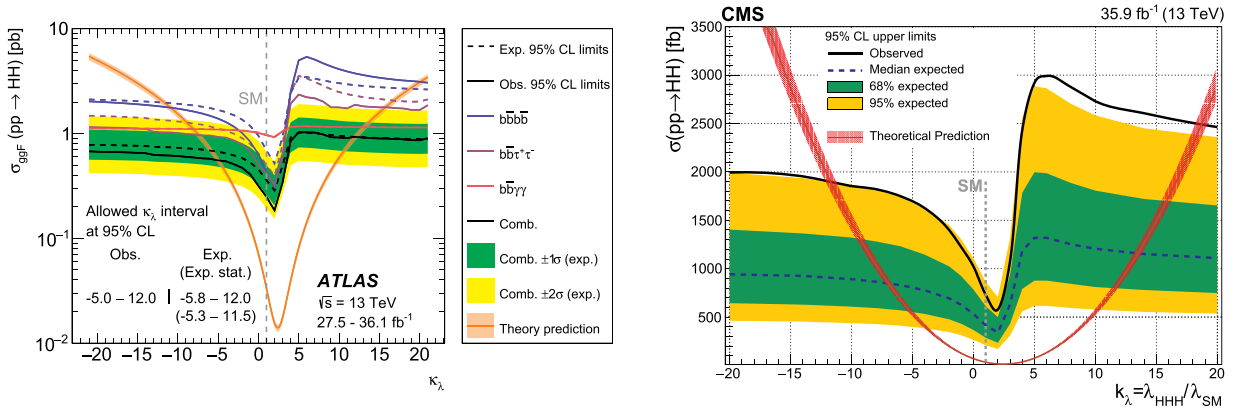

Fig. 11. Cross-section values excluded at 95% confidence level as a function of κ_λ by the ATLAS (left) and the CMS collaborations (right). The result is obtained by combining the limits from different HH final states (see Ref. [49,50]).

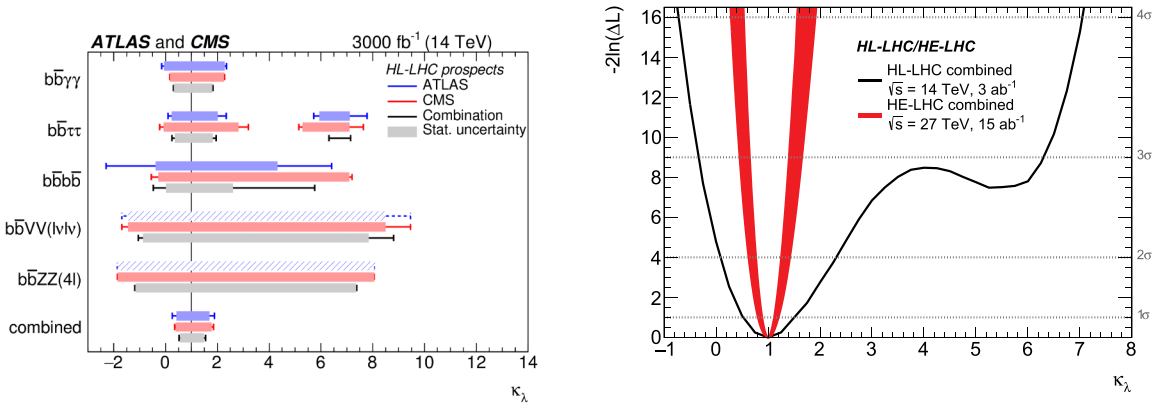

Fig. 12. Left: Expected sensitivity to κ_λ at the HL-LHC by ATLAS and CMS. Right: Expected sensitivity to κ_λ at the HL-LHC and HE-LHC (see Ref. [20]).

4.1. Proton-proton colliders

There are today four major future *pp* collider projects: HL-LHC at $\sqrt{s} = 14$ TeV and with a factor of 10 increae in luminosity compared to LHC [20]; HE-LHC that would increase the$\sqrt{s}$ to 27 TeV within the same tunnel [53]; FCC-pp [54] and CEPC [55] that plan to dig new 50-100 km tunnels and reach $\sqrt{s}$ up to 80-100 TeV.

The LHC HH analyses were extrapolated with different detector assumptions to the increased $\sqrt{s}$, luminosities, harsher background conditions and expected performances of future detectors. The LHC program should increase by roughly a factor of two the already collected luminosity before the end. This would not be sufficient to tackle the SM-like HH production. The HL-LHC program with an expected 10 times larger luminosity seems to have enough sensitivity for a 3σ evidence of SM-like HH production. Unless a significant experimental breakthrough helps, we may not have enough data for a 5σ observation [20]. We shall also be able to measure the κ_λ parameter with a precision of 50% as shown in Fig. 12 (left) and exclude at 95% CL the possibility that the Higgs boson doesn't self-couple. Finally, a lack of HH events in the HL-LHC data would be a strong hint toward a potential difference from the BEH hypothesis.

The real breakthrough for the BEH potential measurement would come from an increase of $\sqrt{s}$ since the HH production cross-section increases quadratically with $\sqrt{s}$. For example, the HE-LHC would provide a measurement of κ_λ at 15% and FCC-hh at 5% precision if we assume similar performance from analyses and techniques as at the HL-LHC [20]. An example of the projection for the HE-LHC is shown in Fig. 12 (right).

4.2. Electron-positron colliders

There are four major e^+e^- collider projects on the market today: circular colliders with energy limited to 365 GeV for the Future Circular Collider at CERN (FCC-ee) [54] and 250 for the Circular Electron-Positron collider in China (CEPC) [55] that could be built before their *pp* equivalents in the same tunnel; The linear collider, ILC [56], with foreseen energy of 250 GeV and a possible upgrade up to 380 GeV or even 500 GeV, and its concurrent project CLIC that may reach the energy of 3 TeV [57].

There are two dominating processes for HH production at e^+e^- colliders: the associated production $e^+e^- \to$ ZHH and VBF $e^+e^- \to HH\nu_e\nu_e$. The cross-sections of both processes are shown in Fig. 13 as a function of $\sqrt{s}$. At least $\sqrt{s} = 400$ GeV is required for a direct observation of HH production. Among all the collider projects to date, only CLIC would reach this energy (excluding the unlikely 500 GeV ILC option). The recent prospects have shown that a precision of O(10%) may be reached on the κ_λ parameter if the

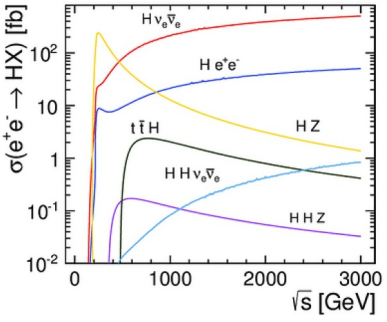

Fig. 13. Production cross-sections of H boson and HH pairs in e^+e^- collisions as a function of $\sqrt{s}$ (see Ref. [58]).

energy of CLIC reaches indeed 3 TeV [58]. All other projects would have to rely on the indirect constraints through the EW loop corrections to the single-Higgs production and Higgs branching fractions. The constraints would be in that case O(100%), which are weaker than the direct ones foreseen from HL-LHC, due to the presence of other contributions to the loop correction from possible BSM operators [59].

5. Conclusions

T he discovery of the Higgs boson at the LHC in 2012 provided us with a strong indication of the nature of the EWSB, the natural phenomena behind the existence of masses for elementary particles. One of the goals of this review was to show that the impression that we understand the EWSB is wrong. We can only guess the shape of the potential that triggers EWSB. In the BEH modeling, the shape of the BEH potential is assumed to be the simplest possible, a quartic polynomial. Until now, we haven't proved by direct measurement that this is true.

The direct measurement of the Higgs boson potential is an absolute priority of the modern HEP scientific program. The HH production is considered as a golden channel since it provides a direct handle on the Higgs self-coupling parameter λ of the BEH potential. Unfortunately, HH production is 1000 times less frequent than the production of a single H boson and its measurement is an extremely challenging task. Due to interference with processes involving the top Yukawa coupling to the H boson, the measurement of λ is even more challenging. The ATLAS and CMS collaborations have invested a significant amount of time and resources in building sophisticated and robust searches for HH production and in reaching a sensitivity of $O(10)$ times the predicted SM cross-section with data collected till 2016. The projections toward the HL-LHC that is the only long-term HEP program approved to date shows that by 2035, the scientific community may have strong hints about the existence of events with a pair of H bosons in the final state. Under that assumption that the BEH potential is rather SM-like, the Higgs self-coupling parameter would then be known at best with a 50% precision. The HL-LHC program would allow excluding at 95% confidence level the possibility of the hypothesis *Higgs boson doesn't couple to itself*. Moreover, a lack of HH events in the HL-LHC data would be a strong hint toward a potential difference from the BEH hypothesis.

All the high energy projects of future colliders proposed to the HEP community try to state the constraint they would bring to the BEH potential. Except for the CLIC project, the e^+e^- colliders are not punchy enough to provide a direct measurement of λ. They can nevertheless constrain the Higgs boson self-coupling indirectly since it contributes to the EW corrections to the single Higgs boson production. On the contrary, all the future *pp* collider programs consider a significant increase of the center-of-mass energy with respect to HL-LHC. They would certainly be able to measure HH production and λ with a precision at least 20% if the BEH potential is SM-like or to exclude the most simple version of the BEH potential.

Acknowledgements

We want to thank Houmani El Mamouni, Philip Baringer, and Bernard Ille for the careful reading and advises on how to improve this review.

References

[1] P. Touboul, G. Métris, M. Rodrigues, Y. André, Q. Baghi, J. Bergé, D. Boulanger, S. Bremer, P. Carle, R. Chhun, B. Christophe, V. Cipolla, T. Damour, P. Danto, H. Dittus, P. Fayet, B. Foulon, C. Gageant, P.-Y. Guidotti, D. Hagedorn, E. Hardy, P.-A. Huynh, H. Inchauspe, P. Kayser, S. Lala, C. Lämmerzahl, V. Lebat, P. Leseur, F.m.c. Liorzou, M. List, F. Löffler, I. Panet, B. Pouilloux, P. Prieur, A. Rebray, S. Reynaud, B. Rievers, A. Robert, H. Selig, L. Serron, T. Sumner, N. Tanguy, P. Visser, Microscope mission: first results of a space test of the equivalence principle, Phys. Rev. Lett. 119 (2017) 231101, https://doi.org/10.1103/PhysRevLett.119.231101.
[2] P. Skands, Introduction to QCD, Proceedings, 2nd Asia-Europe-Pacific School of High-Energy Physics (AEPSHEP 2014): Puri, India, November 0417, 2014, (2013), pp. 341–420, https://doi.org/10.1142/9789814525220_0008,10.23730/CYRSP-2017-002.63. [,63(2017)]
[3] P.W. Higgs, Broken symmetries and the masses of gauge bosons, Phys. Rev. Lett. 13 (1964) 508–509, https://doi.org/10.1103/PhysRevLett.13.508.
[4] F. Englert, R. Brout, Broken symmetry and the mass of gauge vector mesons, Phys. Rev. Lett. 13 (1964) 321–323, https://doi.org/10.1103/PhysRevLett.13.321.
[5] G. Aad, et al., Observation of a new particle in the search for the Standard Model Higgs boson with the ATLAS detector at the LHC, Phys. Lett. B716 (2012) 1–29, https://doi.org/10.1016/j.physletb.2012.08.020.
[6] S. Chatrchyan, et al., Observation of a New Boson at a Mass of 125 GeV with the CMS Experiment at the LHC, Phys. Lett. B716 (2012) 30–61, https://doi.org/10.1016/j.physletb.2012.08.021.
[7] A. Zee, Quantum Field Theory in a Nutshell, Nutshell handbook, Princeton University Press, Princeton, NJ, 2003.
[8] J. Tate, Universe Today, 2009 [Online; accessed 22-July-2019], (https://www.universetoday.com/45317/beta-decay/).
[9] H. Eschrig, A brief introduction to quantum electrodynamics, Fundam. Density Funct. Theory, pp. 160–175. 10.1007/978-3-322-97620-8_9.
[10] G. Rajasekaran, Fermi and the theory of weak interactions, Resonance J. Sci. Educ. 19 (1) (2014) 18–44, https://doi.org/10.1007/s12045-014-0005-2.
[11] S. Weinberg, A model of leptons, Phys. Rev. Lett. 19 (1967) 1264–1266, https://doi.org/10.1103/PhysRevLett.19.1264.
[12] F. Englert, R. Brout, Broken symmetries and the masses of gauge bosons, Phys. Rev. Lett. 13 (1964) 321, https://doi.org/10.1103/PhysRevLett.13.321.
[13] P.W. Higgs, Broken symmetries and the masses of gauge bosons, Phys. Rev. Lett. 13 (1964) 508, https://doi.org/10.1103/PhysRevLett.13.508.
[14] A. Salam, J.C. Ward, On a gauge theory of elementary interactions, Il Nuovo Cimento (1955-1965) 19(1) (1961) 165–170. 10.1007/BF02812723.
[15] M. Banner, R. Battiston, P. Bloch, F. Bonaudi, K. Borer, M. Borghini, J.-C. Chollet, A. Clark, C. Conta, P. Darriulat, L.D. Lella, J. Dines-Hansen, P.-A. Dorsaz, L. Fayard, M. Fraternali, D. Froidevaux, J.-M. Gaillard, O. Gildemeister, V. Goggi, H. Grote, B. Hahn, H. Hnni, J. Hansen, P. Hansen, T. Himel, V. Hungerbhler, P. Jenni, O. Kofoed-Hansen, E. Lanon, M. Livan, S. Loucatos, B. Madsen, P. Mani, B. Mansoulie, G. Mantovani, L. Mapelli, B. Merkel, M. Mermikides, R. Mllerud, B. Nilsson, C. Onions, G. Parrour, F. Pastore, H. Plothow-Besch, M. Polverel, J.-P. Repellin, A. Rothenberg, A. Roussarie, G. Sauvage, J. Schacher, J. Siegrist, H. Steiner, G. Stimpfl, F. Stocker, J. Teiger, V. Vercesi, A. Weidberg, H. Zaccone, W. Zeller, Observation of single isolated electrons of high transverse momentum in events with missing transverse energy at the cern pp collider, Phys. Lett. B 122 (5) (1983) 476–485, https://doi.org/10.1016/0370-2693(83)91605-2.
[16] G. Arnison, A. Astbury, B. Aubert, C. Bacci, G. Bauer, A. Bzaguet, R. Bck, T. Bowcock, M. Calvetti, P. Catz, P. Cennini, S. Centro, F. Ceradini, S. Cittolin, D. Cline, C. Cochet, J. Colas, M. Corden, D. Dallman, D. Dau, M. DeBeer, M. Negra, M. Demoulin, D. Denegri, A.D. Ciaccio, D. Dibitonto, L. Dobrzynski, J. Dowell, K. Eggert, E. Eisenhandler, N. Ellis, P. Erhard, H. Faissner, M. Fincke, G. Fontaine, R. Frey, R. Frhwirth, J. Garvey, S. Geer, C. Ghesquire, P. Ghez, K. Giboni, W. Gibson, Y. Giraud-Hraud, A. Givernaud, A. Gonidec, G. Grayer, T. Hansl-Kozaecka, W. Haynes, L. Hertzberger, C. Hodges, D. Hoffmann, H. Hoffmann,

D. Holthuizen, R. Homer, A. Honma, W. Jank, G. Jorat, P. Kalmus, V. Karimki, R. Keeler, I. Kenyon, A. Kernan, R. Kinnunen, W. Kozanecki, D. Kryn, F. Lacava, J.-P. Laugier, J.-P. Lees, H. Lehmann, R. Leuchs, A. Lvque, D. Linglin, E. Locci, J.-J. Malosse, T. Markiewicz, G. Maurin, T. McMahon, J.-P. Mendiburu, M.-N. Minard, M. Mohammadi, M. Moricca, K. Morgan, H. Muirhead, F. Muller, A. Nandi, L. Naumann, A. Norton, A. Orkin-Lecourtois, L. Paoluzi, F. Pauss, G. Mortari, E. Pietarinen, M. Pimi, A. Placci, J. Porte, E. Radermacher, J. Ransdell, H. Reithler, J.-P. Revol, J. Rich, M. Rijssenbeek, C. Roberts, J. Rohlf, P. Rossi, C. Rubbia, B. Sadoulet, G. Sajot, G. Salvi, G. Salvini, J. Sass, J. Saudraix, A. Savoy-Navarro, D. Schinzel, W. Scott, T. Shah, M. Spiro, J. Strauss, J. Streets, K. Sumorok, F. Szoncso, D. Smith, C. Tao, G. Thompson, J. Timmer, E. Tscheslog, J. Touminiemi, B.V. Eijk, J.-P. Vialle, J. Vrana, V. Vuillemin, H. Wahl, P. Watkins, J. Wilson, C. Wulz, G. Xie, M. Yvert, E. Zurfluh, Experimental observation of lepton pairs of invariant mass around 95 GEV/C2 at the cern sps collider, Phys. Lett. B 126 (5) (1983) 398–410, https://doi.org/10.1016/0370-2693(83)90188-0.

[17] S.F. Novaes, Standard model: an introduction particles and fields, Proceedings, 10th Jorge Andre Swieca Summer School, Sao Paulo, Brazil, February 6-12, 1999, (1999), pp. 5–102.

[18] I. Melo, Higgs potential and fundamental physics, Eur. J. Phys. 38 (2017) 065404, https://doi.org/10.1088/1361-6404/aa8c3d.

[19] P.J. Mohr, D.B. Newell, B.N. Taylor, Codata recommended values of the fundamental physical constants: 2014, Rev. Mod. Phys. 88 (2016) 035009, https://doi.org/10.1103/RevModPhys.88.035009.

[20] M. Cepeda, et al., Higgs Physics at the HL-LHC and HE-LHC (2019).

[21] E.W.N. Glover, J.J. van der Bij, Higgs boson pair production via gluon fusion, Nucl. Phys. B309 (1988) 282–294, https://doi.org/10.1016/0550-3213(88)90083-1.

[22] D. de Florian, et al., Handbook of LHC Higgs cross sections: 4. Deciphering the nature of the Higgs sector, CERN Report, (2016), https://doi.org/10.23731/CYRM-2017-002.

[23] J. Alison, et al., Higgs Boson Pair Production at Colliders: Status and Perspectives, in: B. Di Micco, M. Gouzevitch, J. Mazzitelli, C. Vernieri (Eds.), Double Higgs Production at Colliders Batavia, IL, USA, September 4, 2018-9, 2019, 2019.

[24] C.-Y. Chen, J. Kozaczuk, I.M. Lewis, Non-resonant Collider Signatures of a Singlet-Driven Electroweak Phase Transition, JHEP 08 (2017) 096, https://doi.org/10.1007/JHEP08(2017)096.

[25] I.P. Ivanov, Building and testing models with extended Higgs sectors, Prog. Part. Nucl. Phys. 95 (2017) 160–208, https://doi.org/10.1016/j.ppnp.2017.03.001.

[26] S.P. Martin, A Supersymmetry primer (1997) 1–98. [Adv. Ser. Direct. High Energy Phys.18,1(1998)]. 10.1142/9789812839657_0001.

[27] S. Hartmann, Effective field theories, reductionism and scientific explanation, Stud. Hist. Phil. Sci. B32 (2001) 267–304, https://doi.org/10.1016/S1355-2198(01)00005-3.

[28] J.R. Espinosa, Higgs Effective Field Theory, PoS CORFU2015 (2016) 012, https://doi.org/10.22323/1.263.0012.

[29] A. Carvalho, F. Goertz, K. Mimasu, M. Gouzevitch, A. Aggarwal, On the reinterpretation of non-resonant searches for Higgs boson pairs (2017).

[30] M. Baak, M. Goebel, J. Haller, A. Hoecker, D. Ludwig, K. Moenig, M. Schott, J. Stelzer, Updated status of the global electroweak fit and constraints on new physics, Eur. Phys. J. C72 (2012) 2003, https://doi.org/10.1140/epjc/s10052-012-2003-4.

[31] T.A. Collaboration, The ATLAS experiment at the CERN large hadron collider, J. Instrum. 3 (08) (2008) S08003.

[32] S. Chatrchyan, et al., The CMS experiment at the CERN LHC, JINST 3 (2008) S08004, https://doi.org/10.1088/1748-0221/3/08/S08004.

[33] A.M. Sirunyan, et al., Search for Higgs boson pair production in the $\gamma\gamma b\bar{b}$ final state in pp collisions at $\sqrt{s}$= 13 TeV, Phys. Lett. B788(2019) 7–36. 10.1016/j.physletb.2018.10.056.

[34] M. Aaboud, et al., Search for Higgs boson pair production in the $\gamma\gamma b\bar{b}$ final state with 13 TeV *pp* collision data collected by the ATLAS experiment, JHEP 11 (2018) 040, https://doi.org/10.1007/JHEP11(2018)040.

[35] M. Tanabashi, et al., Review of particle physics, Phys. Rev. D 98 (2018) 030001, https://doi.org/10.1103/PhysRevD.98.030001.

[36] A.M. Sirunyan, et al., Particle-flow reconstruction and global event description with the CMS detector, JINST 12 (2017) P10003, https://doi.org/10.1088/1748-0221/12/10/P10003.

[37] M. Aaboud, et al., Search for resonant and non-resonant Higgs boson pair production in the $b\bar{b}\tau^+\tau^-$ decay channel in *pp* collisions at $\sqrt{s}$ = 13 TeV with the ATLAS detector, Phys. Rev. Lett. 121 (19) (2018) 191801, https://doi.org/10.1103/PhysRevLett.122.089901, 10.1103/PhysRevLett.121.191801. [Erratum: Phys. Rev. Lett.122,no.8,089901(2019)]

[38] A.M. Sirunyan, et al., Search for Higgs boson pair production in events with two bottom quarks and two tau leptons in protonproton collisions at $\sqrt{s}$ =13TeV, Phys. Lett. B778 (2018) 101–127, https://doi.org/10.1016/j.physletb.2018.01.001.

[39] A.M. Sirunyan, et al., Search for resonant and nonresonant Higgs boson pair production in the $b\bar{b}\ell\nu\ell\nu$ final state in proton-proton collisions at $\sqrt{s}$ = 13 TeV, JHEP 01 (2018) 054, https://doi.org/10.1007/JHEP01(2018)054.

[40] G. Aad, et al., Search for non-resonant Higgs boson pair production in the $bb\ell\nu\ell\nu$ final state with the ATLAS detector in *pp* collisions at $\sqrt{s}$ = 13 TeV (2019).

[41] M. Aaboud, et al., Search for Higgs boson pair production in the $b\bar{b}WW^*$ decay mode at $\sqrt{s}$ = 13 TeV with the ATLAS detector, JHEP 04 (2019) 092, https://doi.org/10.1007/JHEP04(2019)092.

[42] A.M. Sirunyan, et al., Search for resonances decaying to a pair of Higgs bosons in the $b\bar{b}q\bar{q}'\ell\nu$ final state in proton-proton collisions at $\sqrt{s}$= 13 TeV, JHEP (2019). Submitted to

[43] M. Aaboud, et al., Search for pair production of Higgs bosons in the $b\bar{b}b\bar{b}$ final state using proton-proton collisions at $\sqrt{s}$ = 13 TeV with the ATLAS detector, JHEP 01 (2019) 030, https://doi.org/10.1007/JHEP01(2019)030.

[44] A.M. Sirunyan, et al., Search for nonresonant Higgs boson pair production in the $b\bar{b}b\bar{b}$ final state at $\sqrt{s}$= 13 TeV, JHEP 04 (2019) 112, https://doi.org/10.1007/JHEP04(2019)112.

[45] M. Aaboud, et al., Search for Higgs boson pair production in the $\gamma\gamma WW^*$ channel using *pp* collision data recorded at $\sqrt{s}$ = 13 TeV with the ATLAS detector, Eur. Phys. J. C78 (12) (2018) 1007, https://doi.org/10.1140/epjc/s10052-018-6457-x.

[46] A. Djouadi, L. Maiani, G. Moreau, A. Polosa, J. Quevillon, V. Riquer, The post-Higgs MSSM scenario: Habemus MSSM? Eur. Phys. J. C73 (2013) 2650, https://doi.org/10.1140/epjc/s10052-013-2650-0.

[47] A. Alves, T. Ghosh, H.-K. Guo, K. Sinha, D. Vagie, Collider and gravitational wave complementarity in exploring the singlet extension of the standard model, JHEP 04 (2019) 052, https://doi.org/10.1007/JHEP04(2019)052.

[48] A. Carvalho, M. Dall'Osso, T. Dorigo, F. Goertz, C.A. Gottardo, M. Tosi, Higgs Pair Production: Choosing Benchmarks With Cluster Analysis, JHEP 04 (2016) 126, https://doi.org/10.1007/JHEP04(2016)126.

[49] G. Aad, et al., Combination of searches for Higgs boson pairs in *pp* collisions at $\sqrt{s}$=13 TeV with the ATLAS detector(2019).

[50] A.M. Sirunyan, et al., Combination of searches for Higgs boson pair production in proton-proton collisions at $\sqrt{s}$= 13 TeV, Phys. Rev. Lett. 122 (12) (2019) 121803, https://doi.org/10.1103/PhysRevLett.122.121803.

[51] M. Aaboud, et al., Observation of Higgs boson production in association with a top quark pair at the LHC with the ATLAS detector, Phys. Lett. B784 (2018) 173–191, https://doi.org/10.1016/j.physletb.2018.07.035.

[52] A.M. Sirunyan, et al., Observation of $t\bar{t}H$ production, Phys. Rev. Lett. 120 (23) (2018) 231801, https://doi.org/10.1103/PhysRevLett.120.231801.

[53] A. Abada, et al., HE-LHC: the high-energy large hadron collider volume, Eur. Phys. J. ST 228 (5) (2019) 1109–1382, https://doi.org/10.1140/epjst/e2019-900088-6.

[54] A. Abada, et al., FCC physics opportunities, Eur. Phys. J. C79 (6) (2019) 474, https://doi.org/10.1140/epjc/s10052-019-6904-3.

[55] The CEPC input for the European Strategy for Particle Physics - Physics and Detector (2019).

[56] H. Baer, et al., The International Linear Collider Technical Design Report - Volume 2: Physics (2013).

[57] L. Linssen, A. Miyamoto, M. Stanitzki, H. Weerts, Physics and detectors at clic: Clic conceptual design report, 2012.

[58] P. Roloff, R. Franceschini, U. Schnoor, A. Wulzer, The Compact Linear e^+e^- Collider (CLIC): Physics Potential (2018).

[59] S. Di Vita, G. Durieux, C. Grojean, J. Gu, Z. Liu, G. Panico, M. Riembau, T. Vantalon, A global view on the Higgs self-coupling at lepton colliders, JHEP 02 (2018) 178, https://doi.org/10.1007/JHEP02(2018)178.